Prefrontal cortex activation and stopping performance underlie the beneficial effects of atomoxetine on response inhibition in healthy and cocaine use disorder volunteers

Peter Zhukovsky [1,2]*, Sharon Morein-Zamir[3]*, Hisham Ziauddeen[1,4], Emilio Fernandez-Egea[1,4], Chun Meng[1,5], Ralf Regenthal[6,7], Barbara J Sahakian[1,5], Edward T Bullmore[1,4,8], Trevor W Robbins[2,5], Jeffrey W Dalley[1,2,5], Karen D Ersche[1,2,5,9†]

*These authors equally contributed to this manuscript

[1]Department of Psychiatry, University of Cambridge, Cambridge, UK

[2]Department of Psychology, University of Cambridge, Cambridge, UK

[3]School of Psychology and Sports Science, Anglia Ruskin University, Cambridge, UK

[4]Cambridgeshire and Peterborough Foundation Trust, Cambridge, UK

[5]Behavioural and Clinical Neuroscience Institute, University of Cambridge, Cambridge, UK

[6]Clinical Pharmacology Department, University of Leipzig, Germany

[7]Leipzig University, Division of Clinical Pharmacology, Rudolf-Boehm-Institute of Pharmacology and Toxicology, Leipzig, Germany

[8]GlaxoSmithKline, Immuno-Inflammation Therapeutic Area Unit, Stevenage UK

[9] Institut for System Neuroscience, University Medical Centre Hamburg-Eppendorf, Hamburg, Germany

† Correspondence: Karen D Ersche, Department of Psychiatry, University of Cambridge, Cambridge, CB2 0SZ

Tel. +44 (0)1223 336587. Fax. +44 (0)1223 338581

Email. ke220@cam.ac.uk

Abstract: 250

Tables: 2

Figures: 3

Supplementary Figures: 4

Supplementary Tables: 3

ABSTRACT

Background: Impaired response inhibition in individuals with cocaine use disorder (CUD) is hypothesised to depend on deficient noradrenergic signalling in cortico-striatal networks. Remediation of noradrenergic neurotransmission with selective norepinephrine reuptake inhibitors such as atomoxetine may therefore have clinical utility to improve response inhibitory control in CUD.

Methods: We carried out a randomised, double-blind, placebo-controlled, crossover study with 26 CUD participants and 28 control volunteers investigating the neural substrates of stop-signal inhibitory control. The effects of a single dose of atomoxetine (40 mg) were compared with placebo on stop-signal reaction time performance and functional network connectivity using dynamic causal modelling.

Results: We found that atomoxetine speeded Go response times in both control and CUD participants. Improvements in stopping efficiency on atomoxetine were conditional on baseline (placebo) stopping performance and were directly associated with increased inferior frontal gyrus activation. Further, stopping performance, task-based brain activation and effective connectivity were similar in the two groups. Dynamic causal modelling of effective connectivity of multiple prefrontal and basal ganglia regions replicated and extended previous models of network function underlying inhibitory control to CUD and control volunteers and showed subtle effects of atomoxetine on prefrontal-basal ganglia interactions.

Conclusions: These findings demonstrate that atomoxetine improves response inhibition in a baseline-dependent manner in control and in CUD participants. Our results emphasize inferior frontal cortex function as a future treatment target due to its key role in improving response inhibition in CUD.

Key words: Impulsivity; Stop Signal Task; fMRI; Cocaine Addiction; Connectivity, DCM, Norepinephrine

INTRODUCTION

Cocaine use disorder (CUD) is exemplified by high levels of impulsivity and impaired response inhibition (1,2). Response inhibition is typically assessed using the stop-signal reaction time (SSRT) task (3–5), with prefrontal hypoactivity a feature of impaired inhibition in stimulant use disorder (6,7). The response inhibitory fronto-striatal network includes the right inferior frontal gyrus (rIFG), dorsomedial prefrontal cortex (dmPFC), putamen and the subthalamic nucleus (STN) (8–11). Neurochemically, response inhibition encompasses dopaminergic and noradrenergic mechanisms operating at distinct cortical and subcortical sites (12,13). Norepinephrine in particular appears to have a preferential contribution to response inhibition in the prefrontal cortex (PFC) (12,14).

Given the prominence of response inhibition difficulties in the conceptualisation of addiction models (7), pharmacological interventions of norepinephrine neurotransmission have been suggested as potentially improving executive inhibitory control in addiction, though its effects in CUD remain to be established (15–17). Atomoxetine is a well-tolerated selective presynaptic norepinephrine transporter blocker (18–20) prescribed for Attention Deficit Hyperactivity Disorder (ADHD), which is also characterised by impulsive behavior and poor response control (21). Acute administration of atomoxetine has been found to improve response inhibition in healthy volunteers and in adult ADHD patients (14,22) and longer-term administration in ADHD has been associated with broader attentional control improvements (23). Additionally, atomoxetine was found to upregulate rIFG during stopping in healthy volunteers (24). Further, atomoxetine ameliorated attentional bias to drug-related cues in CUD participants (25).

However, not all studies on atomoxetine have found performance improvements in stopping or concomitant brain correlates (26–29). A possible reason for this may be baseline-dependent individual differences, whereby only those with worse stopping performance benefit from atomoxetine administration. Two studies on atomoxetine administration in older adults with Parkinson's Disease (PD) found that atomoxetine-related improvement in stopping was associated with baseline performance (30,31). In one of these studies, improvement of response inhibition by atomoxetine was also associated with increased rIFG activation (30). Moreover, these studies pointed to atomoxetine enhancing and even restoring abnormal connectivity within the stopping fronto-striatal network (30,31).

In the current study, we investigated the effects of atomoxetine on inhibitory performance and associated brain function in CUD and healthy control participants. We used pharmacological functional magnetic resonance imaging (fMRI) of the stop-signal task (6,32), expecting CUD participants to show performance impairments that could be remediated by atomoxetine. We hypothesized that changes in fronto-striatal regions subserving stopping would underlie any beneficial effects of atomoxetine. We further aimed to identify effects of atomoxetine on effective connectivity

of the stopping network. To this end, we built on previous dynamic causal modelling (DCM) of the stop-signal task (9), employing this approach on healthy controls and on CUD participants. We extended the network being investigated to encompass the putamen to better assess the interactions between the prefrontal cortex and basal ganglia.

METHODS AND MATERIALS

Participants

A starting sample of twenty-eight healthy participants and twenty-eight individuals who satisfied DSM-IV TR (33) criteria for cocaine dependence, here referred to as cocaine use disorder (CUD) were recruited from drug treatment services by advertisement and word of mouth. Two CUD patients did not complete the task in the scanner and thus were excluded. Healthy control participants were recruited from the Cambridge BioResource volunteer panel (www.cambridgebioresource.org.uk) and had no current or past psychiatric disorders. All participants were screened using the Mini-International Neuropsychiatric Interview (34) and completed the Beck Depression Inventory Version II to record levels of dysphoric mood. We did not assess ADHD but none of our participants had a prior diagnosis of ADHD and had been prescribed stimulants for the treatment of ADHD. Cocaine dependence was verified using the Structured Interview to the DSM-IV (Structured Clinical Interview, SCID (35). Fifteen CUD patients also met the DSM-IV criteria for opioid dependence; 10 of whom were taking methadone or buprenorphine as part of their maintenance therapy. Ten CUD patients also met criteria for tetrahydrocannabinol dependence. Participants were excluded if they 1) had a history of neurological disorder, head or brain injury, history of psychotic disorder, or metabolic disorder, 2) were taking any medication that would interact with atomoxetine such as aripiprazole or bupropion, 3) were pregnant, 4) had MR incompatibilities or 5) had been involved in a clinical trial within the past six months. Urine screens verified recent cocaine use in all CUD patients and were drug negative for all control participants. Additional five CUD patients were excluded from each session due to limited task compliance and race model violations (6), resulting in eight CUD patients precluded from analyses incorporating both sessions (see Supplementary Table 1).

Experimental Procedure and Design

The study followed a randomised, double-blind, placebo-controlled, crossover, balanced design. All participants provided written informed consent, which received ethical approval from National Ethics Committee (12/EE/0519; PI: KD Ersche). Participants received orally either 40mg atomoxetine or a placebo of identical appearance, consistent with previous studies (24,30). At least seven days separated the sessions for each participant, which included a neuropsychological battery and brain imaging (25). Blood samples for plasma were collected 150 minutes after administration (mean 366

ng/mL, standard deviation 200 ng/mL) following established pharmacokinetics immediately after scanning (36,37). Participants underwent structural and functional MRI scanning where they performed the stop-signal task. Generalised linear models (GLM) on SSRT and Go RT were conducted with subject-level random effects (equivalent to mixed-effect Analyses of Variance) to explore the main effects of group (cocaine vs control), drug (atomoxetine vs placebo) and the group-by-drug interaction (*nlme* and *car* packages in RStudio v3.4.1). Age and atomoxetine plasma levels were included as covariates. Regression weights with their respective t and p values are reported. Following the GLM analyses described below, predictors of performance changes due to atomoxetine were explored. ANCOVA models (*aov* package in RStudio, v3.4.1) were fitted to explain the variability in atomoxetine-dependent changes in SSRT and in Go RT.

MRI Acquisition. MRI data were acquired using a Siemens Trio 3T scanner (Erlangen, Germany). Functional images used a whole-brain echo planar image sequence (repetition time, 2000 ms; echo time, 30 ms; flip angle, 78°; 32 slices with 3mm slice thickness and a 0.75mm gap; matrix=64x64; field of view, 192x192mm; 3 x 3mm in-plane resolution; number of volumes ranging between 278 and 305). High resolution T1-weighted gradient echo images were acquired for registration purposes (176 sequential slices of 1mm thickness; repetition time, 2300 ms; echo time, 2.98 ms; flip angle, 9°, FOV, 240x256mm).

Stop-Signal Task. On go trials participants were required to respond with left or right key presses to corresponding left or right arrow stimuli (100ms) (6). On stop trials, a stop signal subsequently appeared (an orange upward arrow, 300 ms) and participants had to cancel their planned response. Left and right arrows were counterbalanced and intermixed, and the delay between go and stop stimuli was adjusted in 50 ms steps from an initial value of 250 ms to achieve 50% successful stopping (38). The task included 48 stop trials and 240 go trials in one block, with stop trials repeating at a later time if participants responded before stop signal onset. Inter-trial-intervals varied randomly between 900 and 1100 ms (39). Participants were instructed to respond as quickly as possible and not to delay responding. Key task outcome measures included mean reaction time (RT) on Go Trials and the SSRT calculated using the integration method with replacement of go omissions (32). Participants who did not meet the assumptions of the race were excluded (6). ΔSSRT was calculated as the difference between SSRT on atomoxetine and SSRT on placebo.

Finally, as part of clinical assessments, participants completed the Beck Depression Inventory (BDI-II), the National Adult Reading Test (NART), an estimate of verbal intelligence, the Obsessive Compulsive Drug Use Scale (OCDUS), Alcohol Use Disorders Identification Test (AUDIT), and the Barratt Impulsivity Scale (BIS-11) (40–45).

MRI Data Processing and Analyses

Pre-processing. FMRI data processing was carried out using FEAT (FMRI Expert Analysis Tool) Version 6.00, part of FSL (FMRIB's Software Library, www.fmrib.ox.ac.uk/fsl). The first five volumes were discarded to achieve steady-state equilibrium. Registration to structural and standard space images was carried out using FLIRT (46–48) and FNIRT (49,50). Pre-processing included motion correction using MCFLIRT (Jenkinson 2002); non-brain removal using BET (51); spatial smoothing using a Gaussian kernel of FWHM 5mm and grand-mean intensity normalisation; high-pass temporal filtering (100s). First level analysis (52) included four regressors of interest: successful stops, failed stops, successful go and error go responses (all other Go-trials) convolved with double-gamma haemodynamic response function. Temporal derivatives were also included for each of the regressors. Successful stops were contrasted with successful go responses (stopping contrast). Twenty-four movement parameters were included as covariates of no interest along with a pre-whitening step.

GLM Analyses. Two GLMs, one for the placebo and one for the atomoxetine drug condition, used one sample whole brain t-tests to identify significant stop-related group mean activations in the control and cocaine groups using FEAT FLAME1 analysis (53). Conjunction analysis tested for overlap between the groups (easythresh_conj.sh, https://warwick.ac.uk/fac/sci/statistics/staff/academic-research/nichols/scripts/fsl). An additional GLM included the difference maps of parameter estimate contrasts for placebo and atomoxetine. Here, one sample t-tests of the atomoxetine versus placebo difference maps were used to evaluate drug effects across subjects and a group-by-drug interaction was tested using independent sample t-tests (CUD vs control) (https://fsl.fmrib.ox.ac.uk/fsl/fslwiki/Randomise/UserGuide).

We also sought to assess whether behavioral effects of atomoxetine were conditional on individual differences in brain activation. To test for associations between drug-related changes in task performance and brain activity, the difference between atomoxetine and placebo in SSRT (ΔSSRT) was added as a covariate to the atomoxetine vs placebo difference GLM. Based on previous findings (24,30), an IFG region of interest (ROI) was applied using the Harvard-Oxford atlas. As significant improvement in Go RT was noted, a parallel yet exploratory analysis was conducted with the difference between drug conditions in Go RT (ΔGoRT) added as a covariate to the go>stop drug difference GLM with primary motor cortex (M1) serving as an ROI (primary motor cortex from the Juelich Atlas). For all analyses, images were thresholded using threshold free cluster enhancement in randomise with 5000 permutations ($z>2.3$, $p<0.05$). Demeaned order of drug vs placebo sessions was included as a second-level covariate of no interest in all GLMs. Group mean activations and placebo-atomoxetine GLMs were conducted using a whole-brain mask while the ΔSSRT and ΔGoRT analyses were conducted within the IFG and M1 masks, respectively.

DCM Analyses. To examine the most likely network identified by group mean GLM maps, and to inspect the directed connectivity in that network, dynamic causal models (DCM; Friston 2003) were built and tested in each group and drug condition in SPM12 (https://www.fil.ion.ucl.ac.uk/spm/software/spm12/). We examined the effective connectivity between well-known nodes of the stopping network that included the IFG, dorsal Anterior Cingulate Cortex (ACC), M1, and STN, building on previous DCM findings (9). We extended the network underlying action initiation and inhibition by adding the putamen, a key node of the indirect cortico-basal ganglia pathway (54,55). The addition of the putamen allowed for the assessment of striatal contributions to response inhibition via the indirect pathway (56) by explicitly modelling its connections with cortical regions such as the dACC and IFG as well as subcortical regions such as the STN.

Full details of the DCM analyses are provided in the Supplementary Information (SI). Briefly, the DCMs allowed us to compare a) fixed connections between the network nodes (DCM.a), b) modulatory effects of the task (successful stop > go contrast) on these connections (DCM.b), c) inputs that drive network activity (Go stimulus presentation on all trials) and d) nonlinear modulatory effects of one node on connectivity between other nodes (DCM.d). A set of 33 models guided by *a priori* hypotheses (Rae et al., 2015) were generated (Figure 3A). Six linear models and five nonlinear models were initially defined to test for linear (DCM.A) and nonlinear (DCM.D) effects (Figure 3A). All models included connections from dACC and from STN to M1, connections from dACC to Putamen and from Putamen to STN. Among the nonlinear models, models A, B and C included interactive effects by the IFG, models D and E included interactive effects by the putamen. The set of 11 models was tested for task modulatory effects (successful stop vs go) at the IFG, the dACC and the putamen, resulting in 3x11=33 models. Bayesian model selection (BMS, Stephan *et al*, 2010) determined the winning models separately in each group in each drug condition. Subject-specific connectivity values from the DCM.A and DCM.B matrices were then extracted for the most likely model for each group by drug condition using Bayesian Model Averaging. The resulting connectivity values from the most likely group model were subsequently subjected to the same subject-level random effects analysis approach as the behavioral performance measures.

RESULTS

Demographic and Behavioral Results

Demographic, clinical and personality measures are reported in Table 1. The participants were well matched in terms of their sex, education level and pattern of alcohol use as reflected by the AUDIT score. CUD patients were younger, had a lower verbal IQ and significantly higher levels of depressed mood on the BDI-II.

Stopping performance is summarized in Table 2. For SSRT there was no main effect of atomoxetine compared with placebo (β=12.6, SE=9.4, t_{44}=1.3, p=0.180), CUD compared with controls (β=5.3, SE=14.7, t_{42}=0.4, p=0.717), nor was there a significant interaction (β=-17.3, SE=12.0, t_{42}=1.4, p=0.151) while controlling for age (β=1.9, SE=0.9, t_{44}=2.1, p=0.038) and plasma atomoxetine levels (p=0.388). For Go RT, there was a significant main effect of drug condition as atomoxetine speeded responding compared with placebo (β=28.5, SE=11.0, t_{44}=2.6, p=0.009), with no main effect of group (β=-27.2, SE=19.3, t_{42}=-1.4, p=0.159) or significant interaction (β=-17.5, SE=14.1, t_{44}=-1.2, p=0.215).

fMRI Results

Whole-brain group mean activations were found in the IFG, dorsal ACC, medial frontal gyrus, parietal and visual areas for the stopping contrast. Conjunction analysis revealed wide-ranging overlap in the above areas activated by both cocaine and control groups in both drug conditions (Figure 1). On placebo, no significant group differences were observed using a whole brain mask. On atomoxetine, CUD patients showed significantly greater activation than controls in the dorsal ACC (peak MNI coordinates [-6, 16, 52], z_{max}=3.89, p=0.002). There were no significant drug effects in either group, nor was there an interaction between group and drug.

In sum, both CUD and control participants showed robust and largely consistent activations in the key nodes of the stopping network regardless of drug condition. Thus, associations with drug-dependent performance differences (ΔSSRT) were assessed across the entire sample. At the whole-brain level no results survived threshold-free cluster-enhancement multiple comparison correction. Using the bilateral IFG mask, we identified a robust cluster of right IFG activation that was associated with improved SSRT performance on atomoxetine (Figure 2A, 2B). This finding was in line with our hypothesis that fronto-striatal activation would be associated with atomoxetine-induced stopping improvements.

Analyses for the go>stop contrast revealed group mean activations in the left precentral gyrus (M1), contralateral to the right-handed task response as would be expected (Supplementary Figure 1). Associations with drug-dependent performance differences (ΔGo RT) showed that within the primary motor cortex (M1) ROI, increased activation in a robust cluster was associated with improved Go RT performance on atomoxetine across all participants (Figure 2C, 2D).

Predictors of changes in performance induced by atomoxetine

To determine the factors predicting changes in performance following atomoxetine administration, mixed-effect generalized linear models (*aov* package) assessed the contribution of placebo performance (“baseline"), plasma atomoxetine, and change in rIFG activation on SSRT improvements on atomoxetine. The rIFG region was defined based on the voxelwise fMRI results in which ΔSSRT

was included as covariate of interest. The full model explained a significant amount of variance in ΔSSRT in all participants (r^2= 0.64, $F_{4,41}$=18.33, p= 1.1e-8).

$$\Delta\text{SSRT} = \beta_1 \times SSRT_{placebo} + \beta_2 \times [\Delta\, rIFG\ activation] + \beta_3 \times [plasma\ Atx] + order$$

Stopping improvement on atomoxetine was predicted by worse baseline stopping performance (beta=-0.32, t_{42}=-3.8, p=4.6e-4), greater activation of rIFG (Figure 2B; beta=-0.19, t_{42}=-5.1, p= 9.5e-6) and by higher levels of plasma atomoxetine (beta=-0.05, t_{42}=-2.3, p=0.025). No significant effects of order were found (p=0.268).

A separate exploratory parallel model was fitted to explain atomoxetine-dependent Go RT improvement. M1 was defined based on the voxelwise fMRI results where ΔGo RT was included as a covariate.

$$\Delta\text{GoRT} = \beta_1 \times GoRT_{placebo} + \beta_2 \times [\Delta\ \text{M1 activation}] + \beta_3 \times [\text{plasma Atx}] + order$$

The full model explained a significant amount of variance in ΔGo RT in all participants (r^2= 0.48, $F_{4,41}$=9.59, p=1.4e-5). Baseline Go RT predicted greater improvement with atomoxetine, with slower responders benefitting more from atomoxetine (beta=-0.22, t_{40}=-2.25, p=0.030). Increases in M1 activation were also associated with faster response execution (Figure 2D, beta=-0.34, t_{40}=-3.8, p=4.4 × 10-4). No significant effects of plasma atomoxetine were found (beta=-0.01, t_{40}=-0.4, p=0.663). No significant effects of order were found (p=0.151).

DCM Results

Overall, DCM connectivity analyses were consistent between the groups and largely replicated previous findings regarding the effective connectivity underlying stopping, though the putamen was not included in previous models (9). Bayesian model selection (Figure 3A, Supplementary Figure 2) indicated the same winning model for both groups on placebo (nonlinear C). Additionally, the winning model was the same for both groups on atomoxetine (linear D). On placebo, the winning model included nonlinear modulation of the hyperdirect dACC-STN connection by the IFG (Figure 3B). In contrast, on atomoxetine this nonlinear modulatory connection was replaced with a fixed connection between the IFG and putamen. Looking at task modulation (the red arrow in Figure 3B), stopping modulated the IFG in controls on placebo, but this changed to the putamen when they were given atomoxetine (DCM.b). Stopping modulated putamen BOLD activity in CUD individuals, regardless of drug condition. This observation is consistent with the expectation that the putamen plays a key role in the stopping network (8–11) and further refines our hypothesis of a fronto-striatal network incorporating the IFG and putamen in modulating stopping performance.

The excitatory and inhibitory connectivity patterns as revealed by the Bayesian Model Averaging in the controls on placebo replicated previous findings with an inhibitory connection from STN to M1

and an excitatory connection between dorsomedial PFC and STN as well as excitatory modulation of this connection by the IFG (9). Extending these results, we show that the putamen provides inhibitory inputs to the STN. To investigate further, mixed effect models assessed the parameters obtained in the Bayesian Model averaging, with no results surviving Bonferroni multiple comparison correction (see SI for further details). Overall, our DCMs replicate and extend an effective connectivity model of prefrontal-basal ganglia interactions in both control and CUD groups and show subtle effects of atomoxetine on the interactions between the IFG and the putamen in both groups.

DISCUSSION

This study investigated the mechanisms underlying the effects of atomoxetine on inhibitory control in CUD and healthy participants. Atomoxetine led to faster response execution across the two groups with no significant effects on stopping latency, in keeping with some previous studies of the effects of atomoxetine on the SSRT task (28,29). We noted prominent and consistent stopping-related group-level BOLD activations in both the placebo and the atomoxetine conditions in both samples with considerable overlap between the groups. These activations encompassed key established nodes of the stopping network including rIFG and dmPFC in addition to striatal and parietal regions (39). Additional connectivity analyses pointed to the same winning model of network architecture in both groups on placebo. The architecture, connections and weights are consistent with those previously found in a cohort of sixteen healthy young adults (9). We extended the connectivity model for response inhibition by introducing and showing the contributions of the putamen which again was consistent across the two groups. Importantly, we also investigated the effect of atomoxetine on effective connectivity. Specifically, whereas on placebo the rIFG modulated the hyper-direct fronto-striatal pathway from the dmPFC to the STN, atomoxetine led to the rIFG modulating the indirect pathway by interacting with the putamen. This change in the network architecture with atomoxetine was found in both groups independently. Taken together, task performance and neural activations point to similar mechanisms of action for atomoxetine across the CUD and control participants.

Individual differences in atomoxetine effects

Importantly, atomoxetine improved stopping performance in a baseline-dependent manner independent from diagnosis, in keeping with findings from a much older cohort of healthy volunteers and PD patients (30,31). Thus, poorer inhibitors benefited the most from atomoxetine compared to placebo. Moreover, this was accompanied by increased rIFG activation such that the greatest improvement in stopping latency was associated with greater upregulation of this region. Higher levels of atomoxetine as detected in the blood were also positively correlated with greater brain activation in the rIFG during successful stopping (24). These results are consistent with the inverted-U modulation by norepinephrine of PFC-mediated cognitive control (58–60). They are reminiscent of findings found not only with atomoxetine but also with methylphenidate which acts on both the

noradrenergic and dopaminergic systems, in accordance with the broader literature of optimal catecholamine levels determining optimal performance (61–63). This also points to the likely utility of placebo inhibitory performance ("baseline") in predicting subsequent effects of atomoxetine on cognitive control across individuals. Larger studies may be more adequately powered to detect group-level benefits to CUD patients driven by those who showed increased rIFG activation and improved stopping performance.

Unexpectedly, atomoxetine also improved response execution compared to placebo. These improvements were found in a baseline-dependent manner, independent from diagnosis. Moreover, faster responding with atomoxetine was positively associated with enhanced activation in primary motor cortex, which is typically activated with response execution (8). Atomoxetine is known to improve attention, but acute administration does not typically promote general response speeding (26,64). Faster response latencies with atomoxetine compared to placebo in the stop-signal task were also reported in ADHD boys (28), suggesting speeding may occur in some situations. The effects on response speeding indicate that atomoxetine facilitated compliance without any concomitant negative effects on stopping, as instructions emphasized to respond as fast as possible and avoid slowing.

Effective connectivity underlying response inhibition and execution

Some of the network connectivity findings are relevant to a general understanding of response inhibition, with others being more specific to its basis in CUD. Present results in controls on placebo provide an important replication and extension of previous DCM findings (9), particularly as such replications are uncommon. Despite some methodological differences, not only was the same winning architecture found, but also there was notable agreement as to the effective connectivity between regions. Specifically, dACC projections to M1 and STN were excitatory, while putamen to the STN and STN to M1 projections were inhibitory (65). Positive modulation of the hyperdirect pathway by rIFG allows for top-down control over response cancellation. Present rIFG-dmPFC connectivity diverges from those previously found (9), possibly due to differences in task instantiation such as their inclusion of no-go trials. Additionally, present results found activation in the dorsal part of the dACC rather than the pre-supplementary motor area, though exact ROI locations appeared spatially adjacent. A subsequent DCM study by the same authors also did not yield similar results, though it was conducted on a considerably older cohort, suggesting that age may modulate stopping network connectivity (31). This would be consistent with the well-established decline in response inhibition from adulthood to older age, with gradual worsening in stopping efficiency (66,67). The present connectivity analyses also extended the stopping network by incorporating an indirect route from the dmPFC to the STN by way of the putamen, as supported by animal and human research in response execution (68). Atomoxetine selectively altered rIFG modulation of dmPFC to STN connectivity for both control and CUD patients, consistent with the notion that it is a key node by which the drug

exerts its influence on response inhibition. Group differences in connectivity were noted, though these did not survive type I error control and were obscured by individual differences. Nevertheless, on the whole the results draw attention to the potential importance of cortico-cortical connectivity in addition to corticostriatal connectivity traditionally associated with impulsivity in CUD (69).

Conclusions and limitations

This study points to baseline-dependent improvements in response inhibition with atomoxetine administration along with concomitant rIFG upregulation in a cohort of CUD patients and in healthy volunteers. CUD patients did not demonstrate impaired stopping or reduced PFC activation compared to controls, contrary to expectations (1,6,70,71). However, CUD patients showed significantly more omissions on Go trials, suggesting a degree of hesitancy manifesting from proactive inhibition (72) being used in this group in view of increased impulsivity (6)(73). Some of the participants were also dependent on opioids and cannabis in addition to cocaine. The stop-signal task is a sensitive measure of response inhibition in stimulant use disorder, with impaired stopping in both clinical and preclinical studies (74–76). Notably, our participants were active cocaine users, and acute cocaine administration has been shown to improve response inhibition (76,77). Alternatively, lack of case-control differences in response inhibition may be due low of power in our sample or differences between the behavioral and the fMRI versions of the stop signal task as some previous studies of CUD patients also report no significant differences in behavioral performance (78–81), suggesting that the evidence for SSRT impairments in CUD patients is inconsistent (75). Therefore, atomoxetine might prove more beneficial in drug abstinent CUD patients in recovery, strengthening response inhibition and preventing relapse. Further, it is possible that participants who chose to undertake a lengthy pharmacological study with multiple visits and perform the task adequately in the scanner exhibit good executive control. In accordance with this notion, alcohol use was not increased in this cohort, though they reported high levels of trait impulsivity, chronic and compulsive drug use. The two groups were also not matched on demographic characteristics, though age was added as a covariate. In principle, atomoxetine may alter the hemodynamic response to neural activity obscuring or confounding any differences detected by fMRI though there is some evidence to counteract this (82). The spatial resolution of fMRI methods restricts precision in regions such as the putamen and STN. To mitigate this, we followed previous methods where possible (9) and used established anatomical masks. The present study used a dose of 40 mg of atomoxetine which is the standard starting therapeutic dose (14). Whilst greater improvements may have been detected with a larger dose, dosage was guided by safety and tolerability considerations.

The results emphasize the nature of response inhibition functioning as existing along a continuum, with considerable overlap between CUD patients and healthy volunteers in the underlying neural network, determining the overall effects atomoxetine has on its nodes and connectivity. Future studies

may explore whether this is the case for other forms of impulsive behaviors such as premature responding also found to be abnormal in stimulant-dependent individuals (73), given the improvements with atomoxetine found in rodent studies (83). The findings also underscore the importance of individual differences within the CUD patients in responding to atomoxetine, as those with worse response control are expected to benefit more from atomoxetine. More generally, the association between rIFG upregulation and successful stopping underscoring the effects of atomoxetine in the present sample supports the development of new interventions that can robustly upregulate rIFG activation in chronic cocaine users.

References

1. Zilverstand A, Huang AS, Alia-Klein N, Goldstein RZ (2018): Neuroimaging Impaired Response Inhibition and Salience Attribution in Human Drug Addiction: A Systematic Review. *Neuron* 98: 886–903.

2. Groman SM, James AS, Jentsch JD (2009): Poor response inhibition: At the nexus between substance abuse and attention deficit/hyperactivity disorder. *Neurosci Biobehav Rev* 33: 690–698.

3. Morein-Zamir S, Robbins TW (2015): Fronto-striatal circuits in response-inhibition: Relevance to addiction. *Brain Res* 1628: 117–129.

4. Ersche KD, Barnes A, Simon Jones P, Morein-Zamir S, Robbins TW, Bullmore ET (2011): Abnormal structure of frontostriatal brain systems is associated with aspects of impulsivity and compulsivity in cocaine dependence. *Brain* 134: 2013–2024.

5. Ersche KD, Jones PS, Williams GB, Turton AJ, Robbins TW, Bullmore ET (2012): Abnormal Brain Structure Implicated in Stimulant Drug Addiction. *Science (80-)* 335: 601–604.

6. Morein-Zamir S, Simon Jones P, Bullmore ET, Robbins TW, Ersche KD (2013): Prefrontal hypoactivity associated with impaired inhibition in stimulant-dependent individuals but evidence for hyperactivation in their unaffected siblings. *Neuropsychopharmacology* 38: 1945–1953.

7. Goldstein RZ, Volkow ND (2011): Dysfunction of the prefrontal cortex in addiction: Neuroimaging findings and clinical implications. *Nat Rev Neurosci* 12: 652–669.

8. Aron AR, Poldrack RA (2006): Cortical and subcortical contributions to stop signal response inhibition: Role of the subthalamic nucleus. *J Neurosci* 26: 2424–2433.

9. Rae CL, Hughes LE, Anderson MC, Rowe JB (2015): The prefrontal cortex achieves inhibitory control by facilitating subcortical motor pathway connectivity. *J Neurosci* 35: 786–94.

10. Chen W, de Hemptinne C, Miller AM, Leibbrand M, Little SJ, Lim DA, *et al.* (2020): Prefrontal-Subthalamic Hyperdirect Pathway Modulates Movement Inhibition in Humans. *Neuron* 106: 579-588.e3.

11. Aron AR, Fletcher PC, Bullmore ET, Sahakian BJ, Robbins TW (2003): Stop-signal inhibition disrupted by damage to right inferior frontal gyrus in humans. *Nat Neurosci* 6: 115–116.

12. Bari A, Mar AC, Theobald DE, Elands SA, Oganya KCNA, Eagle DM, Robbins TW (2011): Prefrontal and Monoaminergic Contributions to Stop-Signal Task Performance in Rats. *J Neurosci* 31: 9254–9263.

13. Robbins TW, Arnsten AFT (2009): The Neuropsychopharmacology of Fronto-Executive Function: Monoaminergic Modulation. *Annu Rev Neurosci* 32: 267–287.

14. Chamberlain SR, Mueller U, Blackwell AD, Clark L, Robbins TW, Sahakian BJ (2006): Neurochemical Modulation of Response Inhibition and Probabilistic Learning in Humans. *Science (80-)* 311: 861–863.

15. Sofuoglu M, Sewell RA (2009): Norepinephrine and stimulant addiction. *Addict Biol* 14: 119–129.

16. Sofuoglu M, Devito EE, Waters AJ, Carroll KM (2013): Cognitive enhancement as a treatment for drug addictions. *Neuropharmacology* 64: 452–463.

17. Quednow BB, Herdener M (2016): Human pharmacology for addiction medicine: From evidence to clinical recommendations. *Progress in Brain Research*, 1st ed., vol. 224. Elsevier B.V. https://doi.org/10.1016/bs.pbr.2015.07.017

18. Swanson CJ, Perry KW, Koch-Krueger S, Katner J, Svensson KA, Bymaster FP (2006): Effect of the attention deficit/hyperactivity disorder drug atomoxetine on extracellular concentrations of norepinephrine and dopamine in several brain regions of the rat. *Neuropharmacology* 50: 755–60.

19. Upadhyaya HP, Desaiah D, Schuh KJ, Bymaster FP, Kallman MJ, Clarke DO, *et al.* (2013): A review of the abuse potential assessment of atomoxetine: A nonstimulant medication for attention-deficit/hyperactivity disorder. *Psychopharmacology (Berl)* 226: 189–200.

20. Bymaster FP, Katner JS, Nelson DL, Hemrick-Luecke SK, Threlkeld PG, Heiligenstein JH, *et al.* (2002): Atomoxetine increases extracellular levels of norepinephrine and dopamine in prefrontal cortex of rat. *Neuropsychopharmacology*.

21. Faraone S V., Asherson P, Banaschewski T, Biederman J, Buitelaar JK, Ramos-Quiroga JA, *et al.* (2015): Attention-deficit/hyperactivity disorder. *Nat Rev Dis Prim Vol* 1.

22. Chamberlain SR, del Campo N, Dowson J, Müller U, Clark L, Robbins TW, Sahakian BJ (2007): Atomoxetine Improved Response Inhibition in Adults with Attention Deficit/Hyperactivity Disorder. *Biol Psychiatry* 62: 977–984.

23. Faraone S V., Biederman J, Spencer T, Michelson D, Adler L, Reimherr F, Seidman L (2005): Atomoxetine and stroop task performance in adult attention-deficit/ hyperactivity disorder. *J Child Adolesc Psychopharmacol* 15: 664–670.

24. Chamberlain SR, Hampshire A, Müller U, Rubia K, del Campo N, Craig K, *et al.* (2009): Atomoxetine Modulates Right Inferior Frontal Activation During Inhibitory Control: A

Pharmacological Functional Magnetic Resonance Imaging Study. *Biol Psychiatry* 65: 550–555.

25. Passamonti L, Luijten M, Ziauddeen H, Coyle-Gilchrist ITS, Rittman T, Brain SAE, *et al.* (2017): Atomoxetine effects on attentional bias to drug-related cues in cocaine dependent individuals. *Psychopharmacology (Berl)* 234: 2289–2297.

26. Nandam LS, Hester R, Wagner J, Cummins TDR, Garner K, Dean AJ, *et al.* (2011): Methylphenidate but not atomoxetine or citalopram modulates inhibitory control and response time variability. *Biol Psychiatry* 69: 902–904.

27. Kasparbauer AM, Petrovsky N, Schmidt PM, Trautner P, Weber B, Sträter B, Ettinger U (2019): Effects of nicotine and atomoxetine on brain function during response inhibition. *Eur Neuropsychopharmacol* 29: 235–246.

28. Cubillo A, Smith AB, Barrett N, Giampietro V, Brammer MJ, Simmons A, Rubia K (2014): Shared and Drug-Specific Effects of Atomoxetine and Methylphenidate on Inhibitory Brain Dysfunction in Medication-Naive ADHD Boys. *Cereb Cortex* 24: 174–185.

29. DeVito EE, Herman AI, Konkus NS, Zhang H, Sofuoglu M (2017): Atomoxetine in abstinent cocaine users: Cognitive, subjective and cardiovascular effects. *Pharmacol Biochem Behav* 159: 55–61.

30. Ye Z, Altena E, Nombela C, Housden CR, Maxwell H, Rittman T, *et al.* (2015): Improving response inhibition in Parkinson's disease with atomoxetine. *Biol Psychiatry* 77: 740–748.

31. Rae CL, Nombela C, Rodríguez PV, Ye Z, Hughes LE, Jones PS, *et al.* (2016): Atomoxetine restores the response inhibition network in Parkinson's disease. *Brain* 139: 2235–2248.

32. Verbruggen F, Aron AR, Band GP, Beste C, Bissett PG, Brockett AT, *et al.* (2019): A consensus guide to capturing the ability to inhibit actions and impulsive behaviors in the stop-signal task. *Elife* 8: 1–26.

33. APA (2000): *American Psychiatric Association: Diagnostic and Statistical Manual of Mental Disorders*.

34. Sheehan D, Lecrubier Y, Sheehan K, Amorim P, Janavs J, Weiller E, *et al.* (1998): The Mini-International Neuropsychiatric Interview (M.I.N.I.): The Development and Validation of a Structured Diagnostic Psychiatric Interview for DSM-IV and ICD-10. *22 J Clin Psychiatry* 59: 22–33.

35. First MB (2002): The DSM series and experience with DSM-IV. *Psychopathology* 35: 67–71.

36. Sauer JM, Ring BJ, Witcher JW (2005): Clinical pharmacokinetics of atomoxetine. *Clin Pharmacokinet* 44: 571–590.

37. Teichert J, Rowe JB, Ersche KD, Skandali N, Sacher J, Aigner A, Regenthal R (2020): Determination of atomoxetine or escitalopram in human plasma by HPLC: Applications in neuroscience research studies. *Int J Clin Pharmacol Ther* 58: 426–438.

38. Logan GD, Schachar RJ, Tannock R (1997): Impulsivity and inhibitory control. *Psychol Sci* 8: 60–64.

39. Whelan R, Conrod PJ, Poline J-B, Lourdusamy A, Banaschewski T, Barker GJ, *et al.* (2012): Adolescent impulsivity phenotypes characterized by distinct brain networks. *Nat Neurosci* 15: 920–925.

40. Patton JH, Stanford MS, Barratt ES (1995): Factor structure of the barratt impulsiveness scale. *J Clin Psychol* 51: 768–774.

41. Saunders JB, Aasland OG, Babor TF, De La Fuente JR, Grant M (1993): Development of the Alcohol Use Disorders Identification Test (AUDIT). *Addiction* 88: 791–804.

42. Dozois DJA, Dobson KS, Ahnberg JL (1998): A psychometric evaluation of the Beck Depression Inventory-II. *Psychol Assess* 10: 83–89.

43. Franken IHA, Hendriks VM, van den Brink W (2002): Initial validation of two opiate craving questionnaires: The Obsessive Compulsive Drug Use Scale and the Desires for Drug Questionnaire. *Addict Behav* 27: 675–685.

44. Nelson HE (1982): The National Adult Reading Test (NART): Test Manual. *Wind UK NFER-Nelson* 124: 0–25.

45. Beck A., Steer R., Brown GK (1996): *Manual for the Beck Depression Inventory-II.*

46. Jenkinson M, Beckmann CF, Behrens TEJ, Woolrich MW, Smith SM (2012): Fsl. *Neuroimage* 62: 782–790.

47. Jenkinson M, Bannister P, Brady M, Smith S (2002): Improved optimization for the robust and accurate linear registration and motion correction of brain images. *Neuroimage* 17: 825–41.

48. Smith SM, Jenkinson M, Woolrich MW, Beckmann CF, Behrens TEJ, Johansen-Berg H, *et al.* (2004): Advances in functional and structural MR image analysis and implementation as FSL. *Neuroimage* 23: 208–219.

49. Andersson JLR, Jenkinson M, Smith SM (2007): Non-linear optimisation. FMRIB technical report TR07JA1. https://doi.org/10.1109/EMOBILITY.2010.5668100

50. Andersson JLR, Jenkinson M, Smith S (2007): Non-linear registration, aka spatial normalization (FMRIB technical report TR07JA2).

51. Smith SM (2002): Fast robust automated brain extraction. *Hum Brain Mapp* 17: 143–55.

52. Woolrich MW, Ripley BD, Brady M, Smith SM (2001): Temporal autocorrelation in univariate linear modeling of FMRI data. *Neuroimage* 14: 1370–1386.

53. Woolrich MW, Behrens TEJ, Beckmann CF, Jenkinson M, Smith SM (2004): Multilevel linear modelling for FMRI group analysis using Bayesian inference. *Neuroimage* 21: 1732–1747.

54. Beeler JA, Petzinger G, Jakowec MW (2013): The enemy within: Propagation of aberrant corticostriatal learning to cortical function in Parkinson's disease. *Front Neurol* 4 SEP: 1–7.

55. Schroll H, Hamker FH (2013): Computational models of basal-ganglia pathway functions: focus on functional neuroanatomy. *Front Syst Neurosci* 7. https://doi.org/10.3389/fnsys.2013.00122

56. Shipp S (2017): The functional logic of corticostriatal connections. *Brain Struct Funct* 222: 669–706.

57. Stephan KE, Penny WD, Moran RJ, den Ouden HEM, Daunizeau J, Friston KJ (2010): Ten simple rules for dynamic causal modeling. *Neuroimage* 49: 3099–3109.

58. Clark KL, Noudoost B (2014): The role of prefrontal catecholamines in attention and working memory. *Front Neural Circuits* 8: 1–19.

59. Aston-Jones G, Cohen JD (2005): An integrative theory of locus coeruleus-norepinephrine function: adaptive gain and optimal performance. *Annu Rev Neurosci* 28: 403–50.

60. Gamo NJ, Wang M, Arnsten AFT (2010): Methylphenidate and atomoxetine enhance prefrontal function through α2-adrenergic and dopamine D1 receptors. *J Am Acad Child Adolesc Psychiatry* 49: 1011–1023.

61. Del Campo N, Fryer TD, Hong YT, Smith R, Brichard L, Acosta-Cabronero J, *et al.* (2013): A positron emission tomography study of nigro-striatal dopaminergic mechanisms underlying attention: Implications for ADHD and its treatment. *Brain* 136: 3252–3270.

62. Eagle DM, Tufft MRA, Goodchild HL, Robbins TW (2007): Differential effects of modafinil and methylphenidate on stop-signal reaction time task performance in the rat, and interactions with the dopamine receptor antagonist cis-flupenthixol. *Psychopharmacology (Berl)* 192: 193–206.

63. Arnsten A, Pliszka S (2011): Catecholamine Influences on Prefrontal Cortical Function: Relevance to Treatment of Attention Deficit Hyperactivity Disorder and Related Disorders. *Pharmacol Biochem Behav* 99: 211–216.

64. Nagashima M, Monden Y, Dan I, Dan H, Tsuzuki D, Mizutani T, *et al.* (2014): Acute neuropharmacological effects of atomoxetine on inhibitory control in ADHD children: A fNIRS

study. *NeuroImage Clin* 6: 192–201.

65. Smith Y, Bevan MD, Shink E, Bolam JP (1998): Microcircuitry of the direct and indirect pathways of the basal ganglia. *Neuroscience* 86: 353–387.

66. Williams BR, Ponesse JS, Schachar RJ, Logan GD, Tannock R (1999): Inhibitory Control Across Lifespan. *Dev Psychol* 35: 205–213.

67. Rey-Mermet A, Gade M (2018): Inhibition in aging: What is preserved? What declines? A meta-analysis. *Psychon Bull Rev* 25: 1695–1716.

68. Calabresi P, Picconi B, Tozzi A, Ghiglieri V, Di Filippo M (2014): Direct and indirect pathways of basal ganglia: A critical reappraisal. *Nat Neurosci* 17: 1022–1030.

69. Dalley JW, Robbins TW (2017): Fractionating impulsivity: neuropsychiatric implications. *Nat Rev Neurosci* 18: 158–171.

70. Li C shan R, Milivojevic V, Kemp K, Hong K, Sinha R (2006): Performance monitoring and stop signal inhibition in abstinent patients with cocaine dependence. *Drug Alcohol Depend* 85: 205–212.

71. Zhang Y, Zhang S, Ide JS, Hu S, Zhornitsky S, Wang W, *et al.* (2018): Dynamic network dysfunction in cocaine dependence: Graph theoretical metrics and stop signal reaction time. *NeuroImage Clin* 18: 793–801.

72. Aron AR (2011): From reactive to proactive and selective control: Developing a richer model for stopping inappropriate responses. *Biol Psychiatry* 69: e55–e68.

73. Zhukovsky P, Morein-Zamir S, Meng C, Dalley JW, Ersche KD (2020): Network failures: When incentives trigger impulsive responses. *Hum Brain Mapp* 1–13.

74. Fillmore MT, Rush CR (2002): Impaired inhibitory control of behavior in chronic cocaine users. *Drug Alcohol Depend* 66: 265–273.

75. Weafer J, Mitchell SH, de Wit H (2014): Recent Translational Findings on Impulsivity in Relation to Drug Abuse. *Curr Addict Reports* 1: 289–300.

76. Fillmore MT, Rush CR, Hays L (2006): Acute effects of cocaine in two models of inhibitory control: Implications of non-linear dose effects. *Addiction* 101: 1323–1332.

77. Garavan H, Kaufman JN, Hester R (2008): Acute effects of cocaine on the neurobiology of cognitive control. *Philos Trans R Soc B Biol Sci* 363: 3267–3276.

78. Li CSR, Huang C, Yan P, Bhagwagar Z, Milivojevic V, Sinha R (2008): Neural correlates of impulse control during stop signal inhibition in cocaine-dependent men.

Neuropsychopharmacology 33: 1798–1806.

79. Ide JS, Hu S, Zhang S, Yu AJ, Li CSR (2015): Impaired Bayesian learning for cognitive control in cocaine dependence. *Drug Alcohol Depend* 151: 220–227.

80. Elton A, Young J, Smitherman S, Gross RE, Mletzko T, Kilts CD (2014): Neural network activation during a stop-signal task discriminates cocaine-dependent from non-drug-abusing men. *Addict Biol* 19: 427–438.

81. Vonmoos M, Hulka LM, Preller KH, Jenni D, Schulz C, Baumgartner MR, Quednow BB (2013): Differences in self-reported and behavioral measures of impulsivity in recreational and dependent cocaine users. *Drug Alcohol Depend* 133: 61–70.

82. Marquand AF, O'Daly OG, De Simoni S, Alsop DC, Maguire RP, Williams SCR, *et al.* (2012): Dissociable effects of methylphenidate, atomoxetine and placebo on regional cerebral blood flow in healthy volunteers at rest: A multi-class pattern recognition approach. *Neuroimage* 60: 1015–1024.

83. Robinson ESJ, Eagle DM, Mar AC, Bari A, Banerjee G, Jiang X, *et al.* (2008): Similar effects of the selective noradrenaline reuptake inhibitor atomoxetine on three distinct forms of impulsivity in the rat. *Neuropsychopharmacology* 33: 1028–1037.

Acknowledgments and Conflicts of Interest

This work was funded by a grant of the Medical Research Council (MR/J012084/1 to TWR, KDE, BJS, ETB) and financially supported by the NIHR Cambridge Biomedical Research Centre and conducted within the Behavioural and Clinical Neuroscience Institute (BCNI).

BJS consults for Cambridge Cognition, Greenfield BioVentures and Cassava Sciences. BJS received funding from the Wallitt Foundation and Eton College and her research is conducted within the NIHR Cambridge Biomedical Research Centre (BRC) Mental Health and Neurodegeneration Themes and the NIHR MedTech and in vitro diagnostic Co-operative (MIC), Cambridge.

TWR consults for Cambridge Cognition, and recently for Greenfield Bioventures, Cassava Sciences, Arcadia, Merck, Sharpe and Dohme, and Lundbeck. He currently receives research grants from Shionogi and GlaxoSmithKline.

CM was supported by a Wellcome Trust grant to KDE (105602/Z/14/Z) and the NIHR Cambridge Biomedical Research Centre. PZ was supported by the Pinsent Darwin studentship from the Department of Physiology, Development and Neuroscience, University of Cambridge. The remaining authors declare no conflict of interests. KDE was supported by an Alexander von Humboldt Fellowship for senior researchers (GBR 1202805 HFST-E), JWD currently receives research grants with Boehringer Ingelheim and GlaxoSmithKline.

We thank all the participants for their contributions to this study, the clinical study officers of the Mental Health Research Network for their help with participant referrals, staff at the NIHR Cambridge Clinical Research Facility and the Wolfson Brain Imaging Centre for their dedicated support throughout this study. We also thank Jean Alrt for support with the study set up, Sanja Abbott for the programming of the paradigm, Claire Whitelock, Ilse Lee and Miriam Pollard for assistance with data collection.

Authors' contributions:

Conception, design: KDE, TWR

Funding: TWR, KDE, BJS, ETB

Data acquisition: KDE

Medial cover and patient care: HZ, EFE

Pharmacokinetics: RR

Data analysis: PZ, SMZ

Interpretation of the data: all authors

Drafting of the article: PZ, SMZ

Critical revision for important intellectual content: all authors

Final approval of the version to be submitted: all authors

Agreement to be accountable for all aspects of the work in ensuring that questions related to the accuracy or integrity of any part of the work are appropriately investigated and resolved: PZ, SMZ, JWD, KDE

Tables and Figures

Table 1. Demographic and psychological assessment data for final Control and CUD groups. Data shown are means (standard deviation).

	Control	CUD	Group statistic (T-value)
Male:Female	27:1	18:0	-
Age (Years)	44.7 (7.4)	38.8 (6.5)	*2.80
Education (Years)	12.8 (2.8)	11.7 (2.2)	1.46
Verbal intelligence (NART)	115.3 (6.7)	104.4 (8.8)	**4.44
Impulsivity (BIS-11 Total)	58.4 (6.8)	74.3 (7.9)	**-6.94
Depression (BDI-II Total)	3.0 (4.4)	16.9 (8.6)	**-6.31
Alcohol use (AUDIT)	3.9 (2.1)	5.6 (6.5)	-1.07
Compulsive drug use (OCDUS)	-	24.4 (8.6)	-
Duration of cocaine use (Years)	-	16.0 (5.6)	-
Plasma atomoxetine ng/ml	293.5 (191.8)	478.4 (159.4)	**-3.48

* p<.01; ** p<.001, Control vs CUD independent samples t-statistics are shown.

Table 2. Performance indices on the Stop Signal Task for final Control and CUD groups. Data shown are means (standard deviations).

	Control		CUD		Group Effect	Atomoxetine Effect
	Plc	Atx	Plc	Atx	$F_{1,44}$	$F_{1,44}$
SSRT (msec)	218 (46)	222 (43)	224 (47)	211 (39)	0.03	0.43
Go RT (msec)	414 (57)	403 (55)	449 (63)	420 (52)	2.73	**7.85
P(Go response|stop)	0.486	0.492	0.466	0.478	2.65	1.30
SSD	171.4	192.7	159.9	183.1	1.19	1.234
P(Go Omissions)	0.009	0.007	0.05	0.05	**11.14	0.09
P(Go Errors)	0.029	0.032	0.05	0.05	*5.34	0.13
GoRT(failed stop)	371.4	363.9	388.5	366.8	0.41	3.61

Plc – placebo, Atx – atomoxetine, * p<.05; ** p<.01

Figure 1. Mean group activation overlap between healthy control and cocaine use disorder (CUD) groups in the placebo and atomoxetine conditions. Overlap maps between the cocaine and control groups were generated in a conjunction analysis of group mean maps using whole-brain cluster-forming threshold of $z=2.3$, $p<0.05$. MNI Z-coordinates are shown below the image slices.

Figure 2. Improved stopping efficiency (stop signal reaction time, SSRT) on atomoxetine is associated with changes in rIFG/rOFC activation (A, B). A bilateral IFG mask (Harvard-Oxford atlas) was used as a region of interest (slices shown at MNI X=50, Z=-12). Improved response execution (reaction times on Go trials, GoRT) on atomoxetine was predicted by changes in primary motor cortex (M1) activity in both groups combined (C, D). A bilateral primary motor cortex mask (Harvard Oxford Atlas) was used as a region of interest (slices shown at MNI X=29, Z=60). T-statistic maps thresholded with threshold-free cluster enhancement (tfce)-corrected $p<0.05$ are shown. ΔrIFG and ΔM1 activations were calculated as the atomoxetine-placebo difference between the average activations (z-maps from first-level GLM analyses) within the regions shown in (A) and (C), respectively.

Figure 3. (A) Fixed connections and driving inputs of dynamic causal models comprising the model space. Six linear models and five nonlinear models were initially defined. The modulatory effects of stopping at 1. IFG, 2. dACC, 3. PUT, resulted in 3x11=33 models. The winning models as revealed by BMS are highlighted for the CUD group (in red) and for the control group (in blue). IFG, inferior frontal gyrus; dACC, dACC dorsal anterior cingulate; STN, subthalamic nucleus; M1, motor cortex; PUT, putamen. Black arrows show driving inputs to the dACC and IFG. Modulatory inputs varied in their location.

Figure 3 (B). Results of Bayesian Model Averaging for control and CUD groups on placebo and atomoxetine. Average parameter estimates for the control and cocaine groups in placebo and atomoxetine conditions in winning DCM model (nonlinear model D on placebo and linear model C on atomoxetine). Bolded connections were significantly different from 0 (one-sample t-tests, uncorrected for multiple comparisons). Autoinhibitory and auto-excitatory connections for IFG, PUT, STN and M1 are not shown. Task modulation locations are highlighted using dotted red arrows and driving inputs to the dACC and IFG are shown in black arrows. (B). IFG, inferior frontal gyrus; dACC, STN, M1, primary motor cortex; PUT, putamen

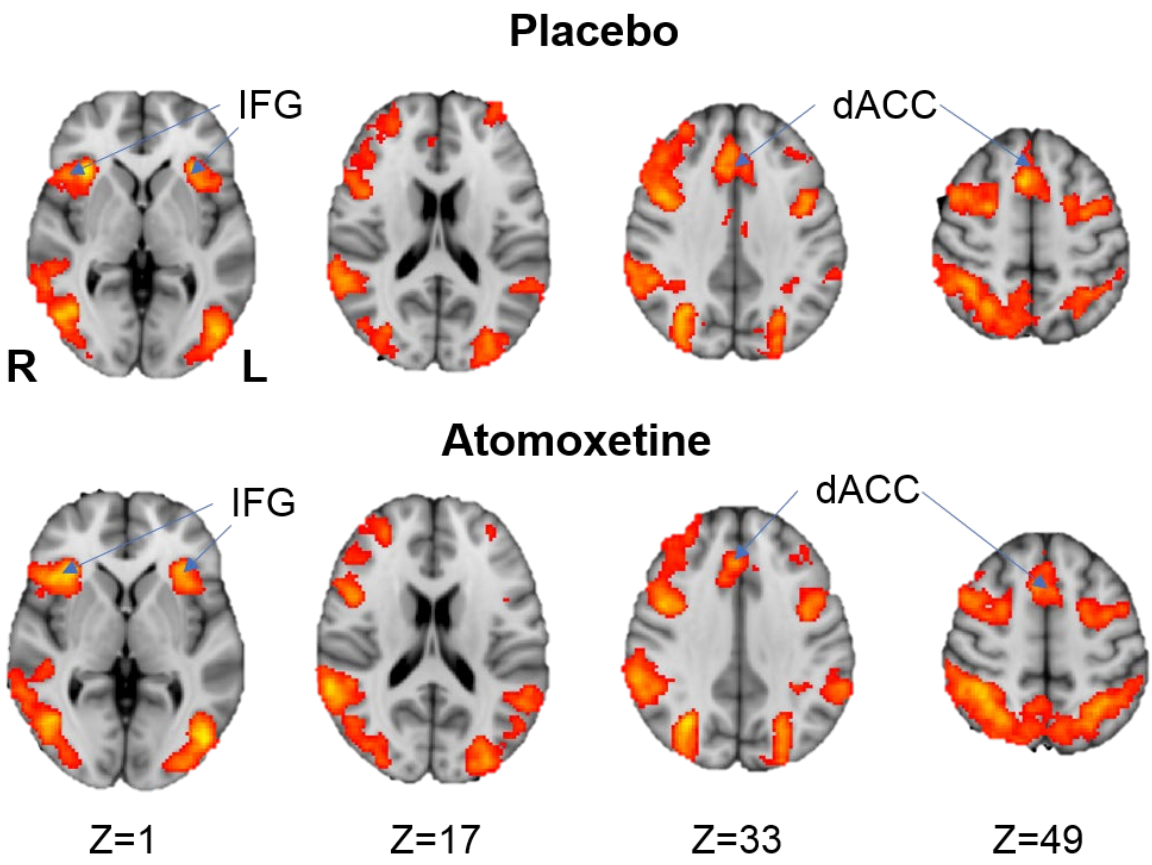
Placebo
IFG
dACC
R
L
Atomoxetine
IFG
dACC
Z=1
Z=17
Z=33
Z=49

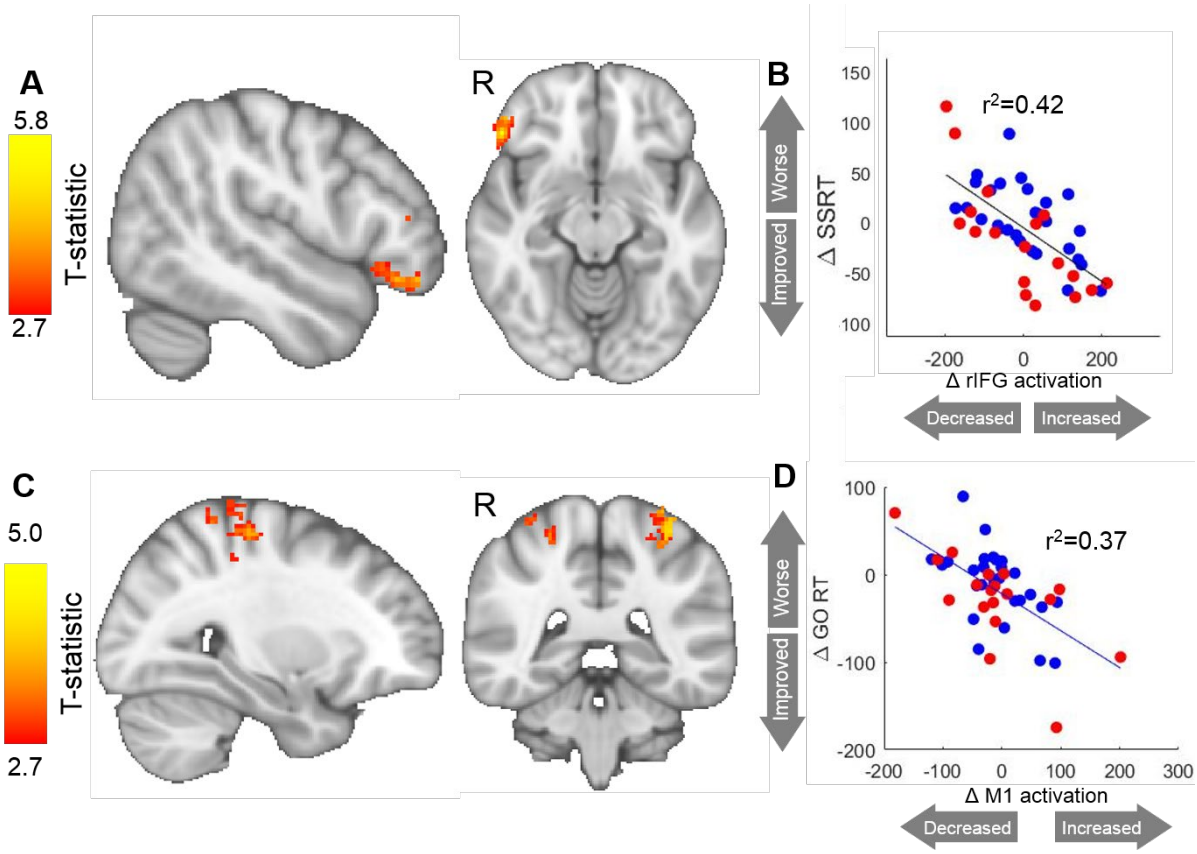
A
5.8
T-statistic
2.7
R
B
Worse
Improved
150
100
50
0
-50
100
r²=0.42
Δ SSRT
-200
0
200
Δ rIFG activation
Decreased
Increased
C
5.0
T-statistic
2.7
R
D
Worse
Improved
100
0
-100
-200
r²=0.37
Δ GO RT
-200
-100
0
100
200
300
Δ M1 activation
Decreased
Increased

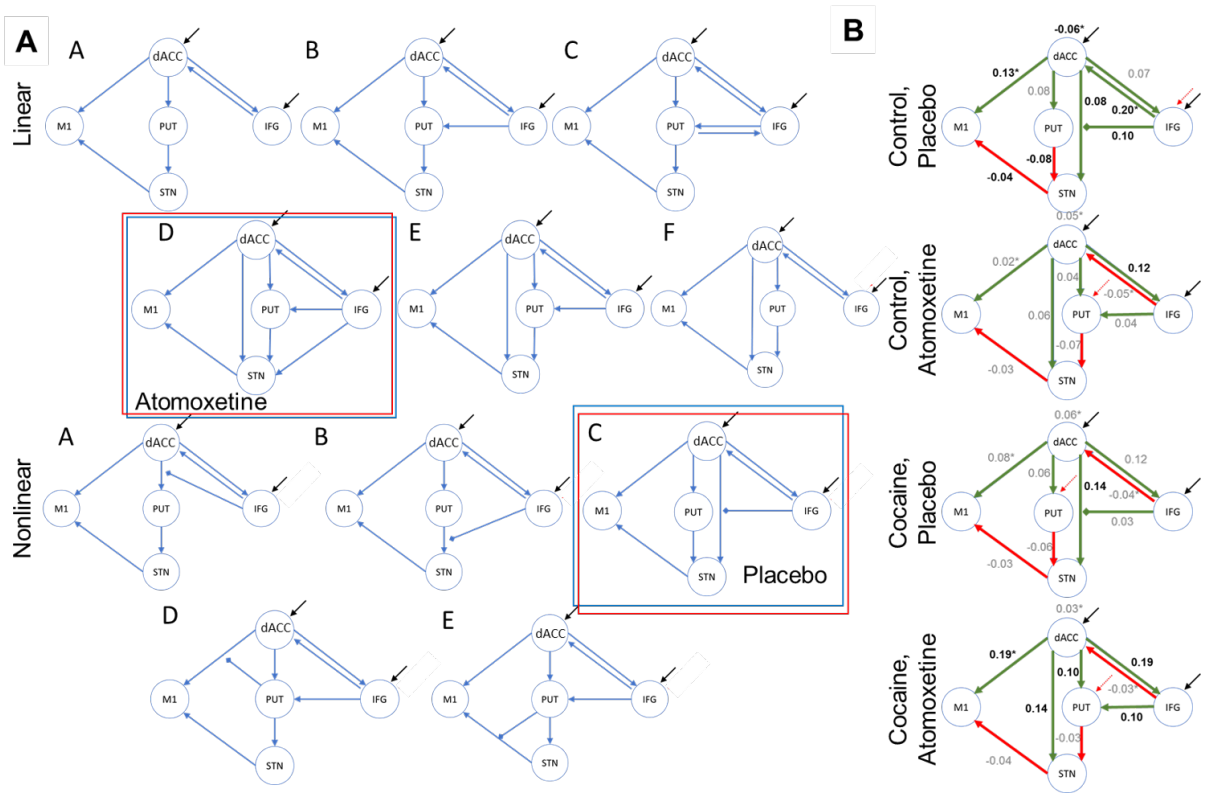
A
Linear
A
B
C
D
E
F
Atomoxetine
Nonlinear
A
B
C
D
E
Placebo
dACC
M1
PUT
IFG
STN
B
Control, Placebo
Control, Atomoxetine
Cocaine, Placebo
Cocaine, Atomoxetine
-0.06*
0.13*
0.07
0.08
0.08
0.20*
0.10
-0.08
-0.04
0.05*
0.02*
0.04
0.12
-0.05*
0.06
0.04
-0.07
-0.03
0.06*
0.08*
0.06
0.12
0.14
-0.04
0.03
-0.06
-0.03
0.03*
0.19*
0.10
0.19
-0.03
0.14
0.10
-0.03
-0.04

Prefrontal cortex activation and stopping performance underlie the beneficial effects of atomoxetine on response inhibition in healthy and cocaine use disorder volunteers –

Supplementary Information

Peter Zhukovsky [1,2]*, Sharon Morein-Zamir[3]*, Hisham Ziauddeen[1,4], Emilio Fernandez-Egea[1,4], Chun Meng[1,5], Ralf Regenthal[6,7], Barbara J Sahakian[1,5], Edward T Bullmore[1,4,8], Trevor W Robbins[2,5], Jeffrey W Dalley[1,2,5], Karen D Ersche[1,2,5,9†]

*These authors equally contributed to this manuscript

Methods

Dynamic Causal Modelling (DCM) Analyses.

DCM allows us to estimate generative models of brain connectivity between a set of regions of interest (ROIs), which can then be compared in terms of their posterior probability given the BOLD timeseries data (1). We examined the effective connectivity between well-known nodes of the stopping network that included the inferior frontal gyrus (IFG), dorsal anterior cingulate (ACC), primary motor cortex (M1), and the subthalamic nucleus (STN), building on previous evidence (2–8).

We extended the network by adding the putamen, a key component of the direct and indirect cortico-basal ganglia pathways (9,10) underlying action initiation and response inhibition.

The DCMs allowed us to assess: a) fixed connections between these nodes (DCM.a), b) modulatory effects of the task (successful stop > go contrast) on these connections (DCM.b), c) inputs that drive network activity (all trials, regardless of trial type or outcome) and d) nonlinear modulatory effects of one ROI on connectivity between other ROIs (DCM.d). A set of 33 models guided by *a priori* hypotheses was compared using Bayesian model selection based on the free-energy bound F, adjusted for model complexity. Further, subject-specific connectivity values can be extracted for the most likely model for each group by drug condition using Bayesian Model Averaging.

Model space included 33 models (Figure 3A), systematically varying in the location of fixed connections (DCM.a), nonlinear modulatory connections (DCM.d) and location of task modulation effects (DCM.b). Fixed connections in linear models tested for systematic differences in the connectivity between the IFG and putamen (linear models A-F). Linear models A-C aimed to test whether ACC-Putamen-STN pathway could replace the hyperdirect pathway (dACC-STN) in stopping; models D-F tested for the role of the IFG given the presence of the hyperdirect pathway and a parallel pathway from the dACC to the STN via the putamen. In particular, we tested whether the IFG-putamen connection was likely, given the data (model D vs model F) and whether an additional projection from the IFG to STN was likely (model E). Nonlinear models examined the addition of nonlinear modulation of the ACC-STN or the ACC-Putamen-STN pathway by the IFG (models A-C). Nonlinear models D and E tested whether putamen may be modulating projections from the ACC to M1 or from the STN to M1. Each of the 11 models had three versions, with task demands (successful stop vs go) modulating the IFG, ACC or Putamen in each model. This resulted in 33 models, though three models failed to converge and were excluded. In each model, all ROIs also had an

autoinhibitory or an autoexcitatory self-connection and all trials provided driving inputs (DCM.c) to the dACC and the IFG following previous definitions of stopping DCMs (8).

Node activations were calculated for each participant. The first Eigenvariate of the BOLD timeseries was extracted from the 1st level analysis. All anatomical masks were taken from the Harvard Oxford cortical and subcortical atlases (11–14). The dorsal ACC and IFG spheres were determined as follows: a search region was first created from the intersection of the significant group mean activation for the successful stop vs go contrast and the anatomical masks of ACC and bilateral IFG (pars opercularis and pars triangularis). This was then masked by a sphere (5 mm radius) of the peak activation from each participant's parameter estimate map for the successful stop vs go contrast. The bilateral motor cortex search region was created from the intersection of the primary motor cortex anatomical mask and significant mean activation for successful go vs stop. Individual-specific spheres (5mm radius) were placed at peak activation for the go vs stop contrast in the search ROI. The putamen sphere (3mm radius) was placed at the subject-specific peak activation in the putamen anatomical region. Finally, STN spheres were created as in Rae *et al.* 2015 by placing spheres of 5mm radius at the specified coordinates (Forstmann *et al*, 2012). Twenty-four extended motion parameters generated in the first level analyses were regressed out of the extracted timeseries and the remaining variability in the BOLD signal was then used to estimate DCMs. Bayesian model selection (BMS, Stephan et al 2009) was used to compare models and model families in each group in each condition by evaluating model posterior probability in a fixed effects analysis. Bayesian model averaging was then used to extract subject-specific connectivity values from the DCM.A and DCM.B matrices for the most likely model for each group in each respective drug condition. These connectivity values were subsequently used in subject-level random effects analyses to examine potential effects of group, drug condition and interaction between group and drug condition. To correct for the number of multiple comparisons, we used the Bonferroni method ($p<0.004$, i.e. 0.05 divided by 12 fixed connections common to all winning models, Figure 3B).

DCM Results and Discussion

Figure S1 summarizes the results of the model selection between thirty DCMs representing competing hypotheses regarding the causal interactions between prefrontal cortical regions and the subcortical response inhibition pathways. The winning models in both groups in both conditions did not differ in terms of fixed connections between ROI pairs (DCM.a). On placebo, but not on atomoxetine, the winning model in both groups included nonlinear modulation of the hyperdirect pathway (ACC to STN) by the IFG (DCM.d). Further, stopping modulated the IFG in the control group in the placebo condition, but the location of stopping modulation changed to the putamen when healthy participants were given atomoxetine. In the Cocaine User Dependent (CUD) group, stopping modulated the putamen activity regardless of drug condition.

Having clarified the presence or absence of connections and modulatory effects, we investigated the connectivity strength within the winning model identified by BMS. Estimating connectivity strength of fixed connections (DCM.a) allows us to assess whether a region is providing excitatory or inhibitory inputs to another region, while nonlinear modulations inform us about increase or reduction in connectivity between two regions by a third modulatory ROI.

The analysis revealed striking similarities to the network architecture previously identified in humans and animals. In particular, the hyperdirect pathway (dACC to STN) as well as the nonlinear modulatory influence of the IFG on the hyperdirect pathway were excitatory. This finding is consistent with a role for the IFG in increasing the excitatory connectivity in the hyperdirect pathway when participants successfully stop a motor response and allowing ACC to activate the STN more strongly. The STN exerts inhibitory control over motor cortex (Redgrave et al 2010) and can thus relay the stopping command it received from the ACC to successfully inhibit the initiated response in the motor cortex.

The dACC provides excitatory inputs to M1, likely facilitating motor action initiation on Go trials, as Go RT performance was related to the dACC-M1 connectivity. Finally, cortical projections to the putamen were excitatory, consistent with models of the direct and indirect pathway (10). The putamen itself provided inhibitory inputs to the STN. It is possible that due to fMRI resolution, the putamen mask included some of the Globus pallidus external, which is thought to have inhibitory projections to the STN.

There were twelve connections (5 autoinhibitory or autoexcitatory connections and 7 fixed or modulatory connections between regions of interest), resulting in twelve mixed models with age and plasma atomoxetine concentration as covariates and subject-level random effects (*nlme* package in R). None of the main or interactive effects were significant at Bonferroni-corrected level, $p<0.004$ (0.05/12). We found a trend interaction between group (cocaine vs control) and drug (atomoxetine vs placebo) on the connectivity between IFG and dACC ($\beta=0.24$, SE=0.12, $t_{44}=2.0$, $p=0.049$), and between dACC and M1 ($\beta=0.18$, SE=0.09, $t_{44}=2.1$, $p=0.042$). Post-hoc tests with FDR correction revealed that the connectivity between IFG and dACC was significantly lower in cocaine dependent participants than in control participants on placebo ($p=0.016$) and decreased in controls ($p=0.006$) but not in cocaine users when they were given atomoxetine. No FDR-corrected differences in connectivity between dACC and M1 were found.

Table S1. Sample size and participant exclusions. Twenty-eight healthy controls were tested on the stop signal task. Twenty-six cocaine dependent active users completed the stop signal task whilst in the scanner. Of these 26 participants, two different subsets of 21 participants were included in the 2nd level comparisons of the group mean activations for the atomoxetine and the placebo conditions. In the placebo condition, five participants were excluded. Exclusion criteria were adopted from (16). In the atomoxetine condition, five participants were also excluded, two of which were the same participants as those who were excluded in the placebo condition. When comparing group mean activations in each condition separately, the maximum number of participants available, namely 21 were used. However, for the interaction analyses between group and condition, only those 18 participants who had fulfilled the task criteria on both the placebo and atomoxetine sessions were included.

	HC	**CUD**	
	Plc, Atx	Plc	Atx
Recruited and tested	28	26	26
fMRI mean group comparison	28	21	21
fMRI Group X Condition	28	18	18
DCM	28	18	18
Behavioural analysis	28	18	18

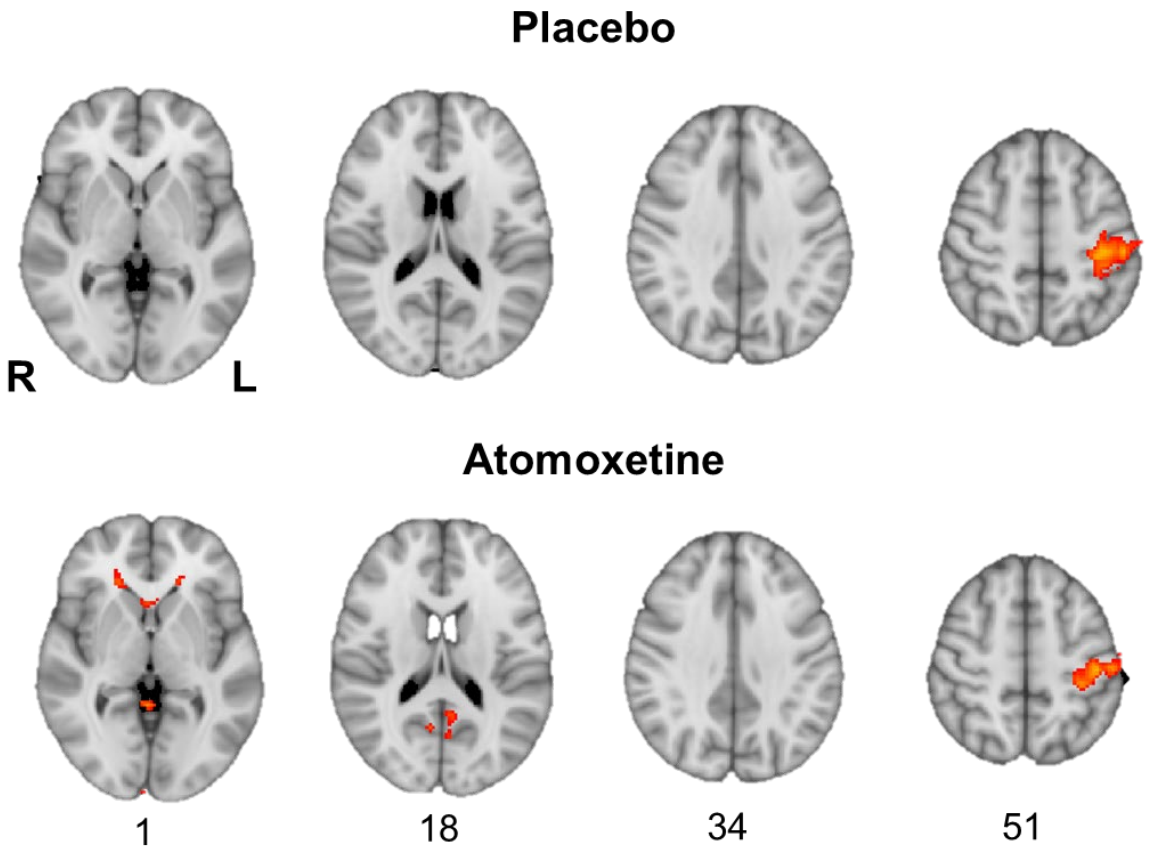

Figure S1. Significant activation maps for the [Successful Go>Successful Stop] contrast showcase the motor cortex activation – precentral/postcentral gyrus. Shown is the conjunction between control and CUD group, cluster corrected with the cluster forming threshold of $z>2.3$ and $p<0.05$.

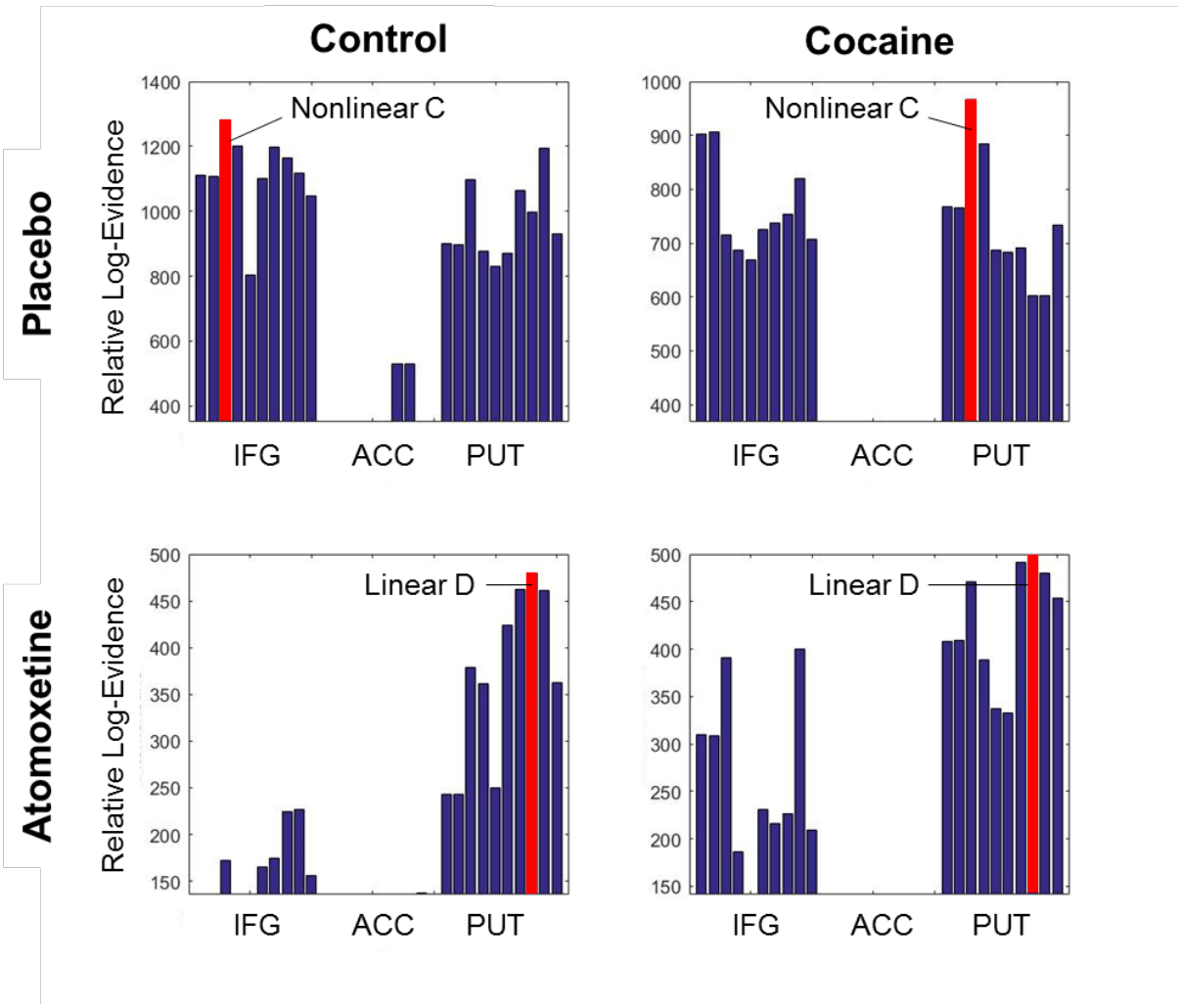

Figure S2. Relative log evidence for each of the thirty models included in the Bayesian model comparison and selection. Models 1-10 are nonlinear models A, B, C, D, E and linear models A, B, C, D, E, F with task modulation of the IFG; models 11-20 are the nonlinear models A, B, C, D, E and linear models A, B, C, D, E, F with task modulation of the ACC; models 21-30 are nonlinear models A, B, C, D, E and linear models A, B, C, D, E, F with task modulation of the putamen. Three models were excluded since they failed to converge for several subjects: nonlinear model D with IFG modulation, nonlinear model E with ACC modulation and nonlinear model E with putamen modulation. The winning models and are highlighted in red. In the placebo condition, nonlinear model C provided the best fit to data from both control and cocaine groups, although stopping modulated the IFG in the controls and the putamen in the cocaine group. In the atomoxetine condition, linear model D with task modulation of the putamen gathered the most evidence in both control and cocaine groups.

Group differences in Go Omissions

In addition to the results reported in Table 1, we show the distribution of the Go omissions in Figure S3. Although a robust, significant difference between CUD patients and controls was found (with increased probability of Go Omissions in CUD), the distribution was heavily skewed towards zero (as shown in Figure S3) and we therefore refrain from testing for linear associations between Go Omissions with task-based stop-signal fMRI data.

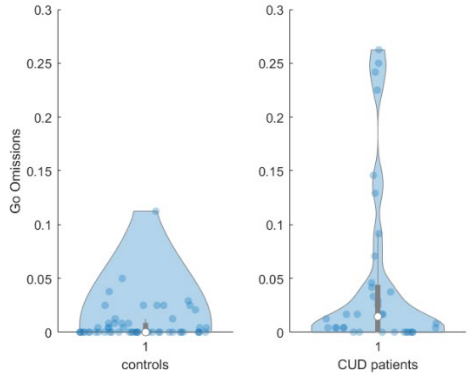

Figure S3. Go omission distribution in healthy controls and CUD patients.

1. Stephan KE, Penny WD, Moran RJ, den Ouden HEM, Daunizeau J, Friston KJ (2010): Ten simple rules for dynamic causal modeling. *Neuroimage* 49: 3099–3109.

2. Aron AR, Fletcher PC, Bullmore ET, Sahakian BJ, Robbins TW (2003): Erratum: Stop-signal inhibition disrupted by damage to right inferior frontal gyrus in humans. *Nat Neurosci* 6: 1329–1329.

3. Floden D, Stuss DT (2006): Inhibitory control is slowed in patients with right superior medial frontal damage. *J Cogn Neurosci* 18: 1843–1849.

4. Nachev P, Wydell H, O'Neill K, Husain M, Kennard C (2007): The role of the pre-supplementary motor area in the control of action. *Neuroimage* 36: 155–163.

5. Jha A, Nachev P, Barnes G, Husain M, Brown P, Litvak V (2015): The frontal control of stopping. *Cereb Cortex* 25: 4392–4406.

6. Cai W, George JS, Verbruggen F, Chambers CD, Aron AR (2012): The role of the right presupplementary motor area in stopping action: Two studies with event-related transcranial magnetic stimulation. *J Neurophysiol* 108: 380–389.

7. Swann NC, Cai W, Conner CR, Pieters TA, Claffey MP, George JS, *et al.* (2012): Roles for the pre-supplementary motor area and the right inferior frontal gyrus in stopping action: Electrophysiological responses and functional and structural connectivity. *Neuroimage* 59: 2860–2870.

8. Rae CL, Hughes LE, Anderson MC, Rowe JB (2015): The prefrontal cortex achieves inhibitory control by facilitating subcortical motor pathway connectivity. *J Neurosci* 35: 786–94.

9. Beeler JA, Petzinger G, Jakowec MW (2013): The enemy within: Propagation of aberrant corticostriatal learning to cortical function in Parkinson's disease. *Front Neurol* 4 SEP: 1–7.

10. Schroll H, Hamker FH (2013): Computational models of basal-ganglia pathway functions: focus on functional neuroanatomy. *Front Syst Neurosci* 7. https://doi.org/10.3389/fnsys.2013.00122

11. Goldstein JM, Seidman LJ, Makris N, Ahern T, O'Brien LM, Caviness VS, *et al.* (2007): Hypothalamic Abnormalities in Schizophrenia: Sex Effects and Genetic Vulnerability. *Biol Psychiatry* 61: 935–945.

12. Desikan RS, Ségonne F, Fischl B, Quinn BT, Dickerson BC, Blacker D, *et al.* (2006): An automated labeling system for subdividing the human cerebral cortex on MRI scans into gyral based regions of interest. *Neuroimage* 31: 968–980.

13. Makris N, Goldstein JM, Kennedy D, Hodge SM, Caviness VS, Faraone S V., *et al.* (2006): Decreased volume of left and total anterior insular lobule in schizophrenia. *Schizophr Res* 83: 155–171.

14. Frazier JA, Chiu S, Breeze JL, Makris N, Lange N, Kennedy DN, *et al.* (2005): Structural brain magnetic resonance imaging of limbic and thalamic volumes in pediatric bipolar disorder. *Am J Psychiatry* 162: 1256–1265.

15. Forstmann BU, Keuken MC, Jahfari S, Bazin PL, Neumann J, Schäfer A, *et al.* (2012): Cortico-subthalamic white matter tract strength predicts interindividual efficacy in stopping a motor response. *Neuroimage* 60: 370–375.

16. Morein-Zamir S, Simon Jones P, Bullmore ET, Robbins TW, Ersche KD (2013): Prefrontal hypoactivity associated with impaired inhibition in stimulant-dependent individuals but evidence for hyperactivation in their unaffected siblings. *Neuropsychopharmacology* 38: 1945–1953.